Heat Mass Transfer (2017) 53:1863–1871
DOI 10.1007/s00231-016-1946-7

ORIGINAL

# Investigation of drying kinetics of tomato slices dried by using a closed loop heat pump dryer

**Salih Coşkun[1] · İbrahim Doymaz[2] · Cüneyt Tunçkal[3] · Seçil Erdoğan[4]**

Received: 25 March 2016 / Accepted: 11 November 2016 / Published online: 19 November 2016


**Abstract** In this study, tomato slices were dried at three different drying air temperatures (35, 40 and 45 °C) and at 1 m/s air velocities by using a closed loop heat pump dryer (HPD). To explain the drying characteristics of tomato slices, ten thin-layer drying models were applied. The drying of tomato slices at each temperature occurred in falling-rate period; no constant-rate period of drying was observed. The drying rate was significantly influenced by drying temperature. The effective moisture diffusivity varied between $8.28 \times 10^{-11}$ and $1.41 \times 10^{-10}$ $m^2/s$, the activation energy was found to be 43.12 kJ/mol. Besides, at the end of drying process, the highest mean specific moisture extraction ratio and coefficient of performance of HPD system were obtained as 0.324 kg/kWh and 2.71, respectively, at the highest drying air temperature (45 °C).

## List of symbols

| | |
|---|---|
| $COP_{hp}$ | Coefficient of performance of heat pump |
| $COP_{sys}$ | Coefficient of performance of whole system |
| $\dot{W}_{comp}$ | Power consumption of compressor (kW) |
| $\dot{Q}_{cd}$ | The amount of heat transferred to drying air (kW) |
| $\dot{W}_{fan}$ | Power consumption of fan (kW) |
| $\dot{m}_a$ | Mass flow rate of drying air (kg/s) |
| $h_A$ | Specific enthalpy of drying air at condenser outlet (kJ/kg) |
| $h_E$ | Specific enthalpy of drying air at condenser inlet (kJ/kg) |
| $SMER$ | Specific moisture extraction ratio (kg/kWh) |
| $\dot{m}_w$ | Mass flow rate of water extracted from product (kg/h) |
| MR | Moisture ratio |
| $M_t$ | Moisture ratio at any time |
| $M_o$ | Initial moisture ratio |
| $M_e$ | Equilibrium moisture ratio |
| DR | Drying rate |
| $MR_{exp,i}$ | Experimental dimensionless moisture ratio |
| $MR_{pre,i}$ | Predicted dimensionless moisture ratios |
| $N$ | Number of observations |
| $z$ | Number of constants |
| $D_{eff}$ | Effective moisture diffusivity ($m^2/s$) |
| $t$ | Time (s) |
| $L$ | Half-thickness of samples (m) |
| $n$ | Number of arguments and summation index |
| $D_0$ | Pre-exponential factor ($m^2/s$) |
| $E_a$ | Activation energy (kJ/mol) |
| $R$ | Universal gas constant (kJ/mol K) |
| $T$ | Drying air temperature (K) |
| $u_n$ | Error rates |
| $U_F$ | Total uncertainty |

## Substcripts

| | |
|---|---|
| a | Air, constant in drying models |
| w | Water |
| comp | Compressor |
| fan | Fan |
| i | Inlet |
| o | Outlet |

✉ Salih Coşkun
scoskun1968@gmail.com

[1] Electric and Energy Department, Air Conditioning and Refrigeration Technology Program, Vocational School of Technical Science, 16059 Bursa, Turkey

[2] Department of Chemical Engineering, Yildiz Technical University, 34210 Esenler, Istanbul, Turkey

[3] Electric and Energy Department, Air Conditioning and Refrigeration Technology Program, Yalova Community College, Yalova University, 77100 Yalova, Turkey

[4] Atatürk Horticultural Central Research Institute, 77102 Yalova, Turkey

| | |
|---|---|
| hp | Heat pump |
| sys | System |
| b | Constant in drying models |
| c | Constant in drying models |
| g | Coefficient in drying models, 1/s |
| k | Coefficient in drying models, 1/s |
| n | Constant in drying models |

## 1 Introduction

There are many investigations on hot air drying, vacuum drying, freezing drying and heat pump drying (HPD) systems to improve drying quality and energy efficiency. The HPD system is the most advanced system because of lowest energy consumption [12, 20]. According to various studies, color and flavor quality of agricultural products dried by HPD system were better than products dried by conventional dryer with hot air [31, 35–37]. There are also various studies related with drying under modified atmosphere. Under the modified atmosphere it was observed that, the quality of products was obtained very well and values of color and C vitamin were also protected [22, 39]. There are many studies about dried agricultural products by using HPD system. Mango and papaya [3, 35, 37], tomato [5, 33], herbs such as ginseng, Echinacea [29], hazelnut [4], fruits such as kiwi, avocado and bananas [6, 10, 11], pepper [28], apple [7, 38], grape [2], and mushroom [25], etc., can be given as examples.

Tomato (*Lycopersicon esculentum* Mill) is the world's most common commercially produced vegetable. It is grown worldwide on a variety of soils due to climatic conditions. The world tomato production reached 163,963,770 metric tons, and Turkey produced about 11,820,000 metric tons of tomatoes in the 2013 [18]. China, India, United States, Turkey and Egypt are the leading tomato-growing countries. Tomato drying has been investigated to a great extent and a lot of data are available in literature. Zanoni et al. [40] studied the drying the samples of tomatoes, halved, in a conventional dryer and they studied the effect of drying conditions of the lycopene content of the tomato. El-Sebaii et al. [15] performed locally solar dryer with indirect natural convection to dry tomato, onion, fig and grape. They studied experimentally and theoretically the correlation between the constant K and the drying temperature of the product in a thin layer. Sacilik et al. [34] studied experimentally solar drying curves of tomato cut in half and distributed in a solar dryer under atmospheric conditions of Ankara (Turkey) and they compared them to the way drying in open air. Doymaz [14] studied the effect of treatment on drying kinetics of tomatoes cut in half and distributed on shelves of a forced convection dryer at temperatures of 55, 60, 65 and 70 °C by using electrical resistors passing perpendicularly through the grids. Hasturk Sahin et al. [21] studied that the effects of drying methods, such as hot-air drying (at 65, 75 and 85 °C drying temperatures), sun drying, vacuum drying and freeze drying, and pretreatments, namely dipping into 1% ascorbic acid + 1% citric acid and dipping into 2% sodium metabisulphite after 2% ethyl oleate + 4% potassium carbonate solution application on lycopene retention and colour properties of dried tomato slices. However, there is no information for drying of tomato slices in the closed loop heat pump dryer. The purpose of the present work was to investigate the effect of air temperature on the drying characteristics of tomato slices in the closed loop HPD system, to fit the experimental data to ten thin-layer models, and to calculate the effective moisture diffusivity and activation energy.

## 2 Materials and methods

### 2.1 Sample preparation

In this study, 2.1 kg peeled tomato slices at 7 mm thickness and 40 ± 2 mm diameter were dried using a HPD designed and manufactured in the Yalova University Air Conditioning and Refrigeration Technology Program Laboratory. The tomato moisture content was determined by drying in a moisture analyzer. A 7 mm tomato sample weighing 5 g was heated at 70 °C for 18 min until reaching the equilibrium point. The initial moisture content on a dry basis of the tomato slices dried in the chamber was determined as 15.667 g water/g dry matter. The results of the experiments showed the tomato slices were dried until the moisture content reached 0.865 g water/g dry matter. The mass of the dried product was measured using an electronic scale placed inside the drying chamber. The experiments were carried out at 1 m/s air velocity and at three different drying chamber temperatures (35, 40 and 45°C).

### 2.2 Experimental set-up

The designed drying system consisted of a heat pump, a fan, a channel system and a 0.60 × 0.60 × 0.60 $m^3$ drying chamber in which there are drying trays with holes 0.12 mm × 0.1 mm in size of 46 cm long and 42 cm width. The HPD experimental set-up used a circulating R410A refrigerant fluid and an internal and an external condenser serially connected to each other. The HPD system was designed so that the drying air was circulated within a closed-loop conduit system using an axial fan and outside air was not taken in during drying. The drying air (E) entering from the internal condenser is warmed by the heat of the refrigerant and enters the drying chamber (A). The heat-providing refrigerant is condensed (3) and was sent

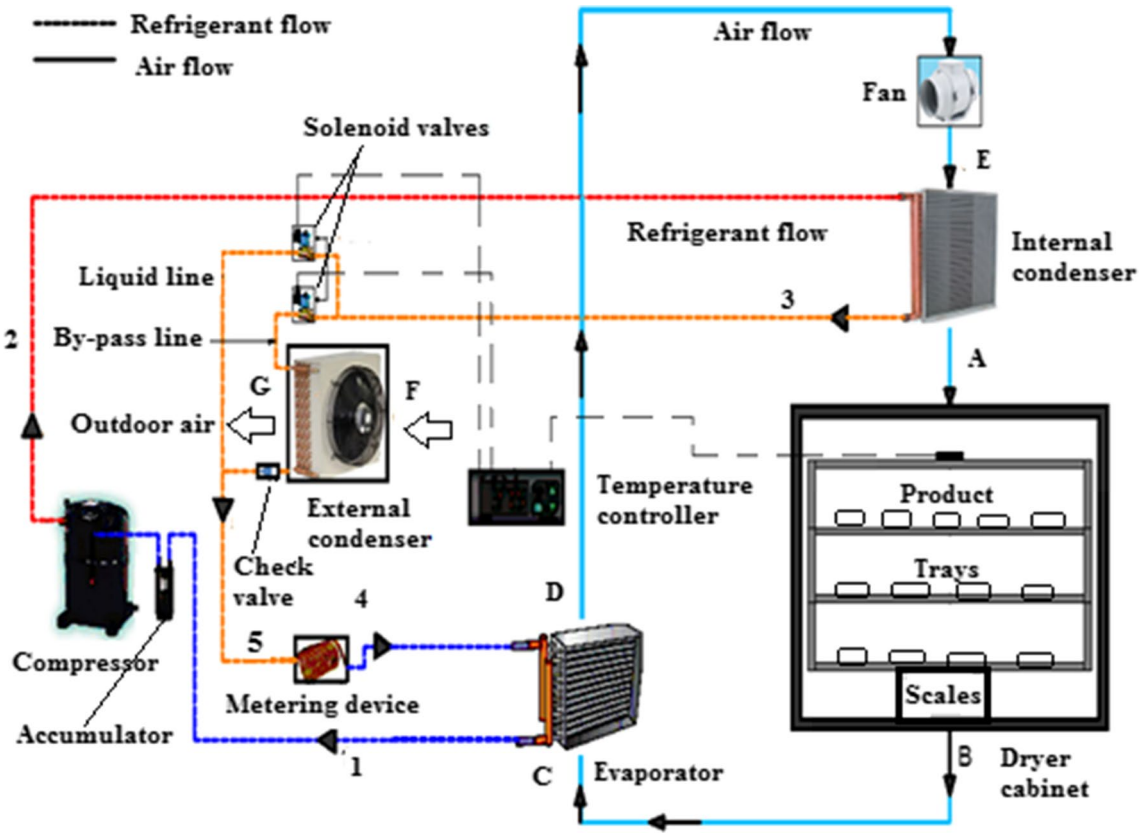


**Fig. 1** Experimental set-up

**Table 1** Technical specifications of heat pump components

| Components | Technical specifications |
|---|---|
| Compressor | Rotary type, cylinder volume 8.6 $cm^3$, nominal power 750 W |
| Evaporator | Aluminum finned tube heat exchanger |
| | Total heat transfer area, 278 $m^2$ |
| Internal condenser | Aluminum finned tube heat exchanger |
| | Total heat transfer area, 3.60 $m^2$ |
| External condenser | Aluminum finned tube heat exchanger |
| | Total heat transfer area, 1.56 $m^2$ |
| Internal condenser fan | Axial type (nominal power 50 W) |
| External condenser fan | Axial type (nominal power 33 W) |
| Metering device (capillary tube) | 1 m length and $1.5 \times 10^{-3}$ m diameter |
| Refrigerant | Freon—410a |

to the evaporator by passing through the capillary tube under reduced pressure (4). Upon contact with the products placed in the tray, the drying air, having increased temperature and lower relative humidity, via heat and mass transfer, takes the moisture within the structure of the product and leaves the drying chamber with higher relative humidity (B). Then, the drying air with high relative humidity is passed through the heat pump evaporator (C–D) in order to be used again. The drying air with the moisture removed from the product, having a temperature below the dew point, condenses while passing over the evaporator tubes containing circulating refrigerant. Thus, by removal of the moisture, the drying air is made available for the drying operation; however, the drying air is cooled somewhat in the process. Inside the evaporator tubes, the circulating refrigerant, upon absorbing the heat from the drying air, evaporates (1) and is absorbed by the compressor, putting pressure on the condenser (2).

**Table 2** Measurement devices

| Measured quantity | Measurement device | Measurement range | Accuracy |
|---|---|---|---|
| Mass of product | Electronic scale | 0–70 kg | ±2 g |
| Drying air velocity | Rotating anemometer | 0.1–10 m/s | ±0.1 m/s |
| Drying air temperature and relative humidity | Hygro-thermometer | 0–100% RH, −40 to 80 °C | ±2% RH, ±0.4 °C |
| Indoor air temperature and relative humidity | Thermo-anemometer | −20 to +70 °C, 0.4–20 m/s | ±0.5 °C, ±0.2 m/s |
| Power consumption of compressor and fans | Electrical power meter | 150–300 V | 0.5 s/day |
| Pressures | Electronic manifold | 0–50 bar | ±0.1 bar |
| Heat pump operating temperatures | Four channel datalogging thermometer | −40 to 250 °C | ±0.5 °C |
| Drying chamber temperature | Electronic thermostat | −50 to +130 °C | ±0.1 °C |

**Table 3** Mathematical models used to describe the drying kinetics of tomato slices

| Model name | Model |
|---|---|
| Lewis | $MR = \exp(-kt)$ |
| Henderson and Pabis | $MR = a\exp(-kt)$ |
| Logarithmic | $MR = a\ \exp(-kt) + c$ |
| Verma et al. | $MR = a\ \exp(-kt) + (1-a)\exp(-gt)$ |
| Page | $MR = \exp(-kt^n)$ |
| Midilli et al. | $MR = a\exp\left(-kt^n\right) + bt$ |
| Parabolic | $MR = a\ + bt + ct^2$ |
| Wang and Singh | $MR = 1\ + at + bt^2$ |
| Weibull | $MR = \exp\left(-\left(\frac{t}{b}\right)^a\right)$ |
| Aghbashlo et al. | $MR = \exp\left(-\left(\frac{at}{1+bt}\right)\right)$ |

The HPD system is shown in Fig. 1 and the technical characteristics of the elements constituting the HPD system are given in Table 1.

In this system, an electronic scale placed in the drying chamber was used to measure the mass of the product. The temperature of the circulating drying air and relative humidity values in the system were recorded via a data acquisition device. The HPD system suction and discharge pressure values were measured using an electronic manifold, and the refrigerant temperatures were measured by thermocouple elements mounted on the pipe surface. The values of the power consumed by the compressor and by the system as a whole were measured and continuously recorded using an electrical power meter. All the recorded data were transferred to the Microsoft Excel 2010 program and the necessary calculations were performed. The measurement devices used during the experiments and their technical specifications are given in Table 2.

Measurements were performed to evaluate the efficiency of the HPD system. Before starting the experiments, the system was run for at least 30 min in order to reach steady-state conditions. During the experiments, the drying chamber temperature was maintained at 35, 40 and 45 °C using a thermostat which is controlled by two solenoid valves. One of them was placed at the by-pass line, while the other was placed at the liquid line, as seen in Fig. 1. The drying chamber temperature was measured by an electronic thermostat whose sensing bulb was placed in the drying chamber. When the drying chamber temperature reached the set value, the thermostat closed the solenoid valve at the liquid line, as it opened the other at the by-pass line and thus, the external condenser was also activated with the internal condenser. When the drying chamber temperature fell to the predefined differential temperature value (about ±0.5 °C), then the thermostat closed the by-pass solenoid valve and opened the other one, and so deactivating the external condenser. It can be seen that the external condenser was less activated at the higher drying chamber temperature.

## 3 Analyses

### 3.1 Mathematical modelling of HPD system

Coefficient of performance of HPD system is defined by two ways; specific moisture extracted ratio (SMER) known as water extracted from product per consumed energy and coefficient of performance (COP) known as heat given drying air through the condenser per consumed energy at compressor [24]. COP value for whole system is determined as Eq. (1).

$$COP_{sys} = \frac{\dot{Q}_{cd}}{\dot{W}_{comp} + \dot{W}_{fan,i} + \dot{W}_{fan,o}} \tag{1}$$

Here, amount of heat given drying air is calculated from Eq. (2).

$$\dot{Q}_{cd} = \dot{m}_a(h_A - h_E) \tag{2}$$

SMER is calculated as follow,

$$SMER = \frac{\dot{m}_w}{\dot{W}_{comp} + \dot{W}_{fan,i} + \dot{W}_{fan,o}} \tag{3}$$

### 3.2 Mathematical modelling of drying process

To evaluate the characteristics of tomato slices drying, it is important for modelling the drying process. Therefore, the data derived from drying of tomato slices was fitted with ten different drying models (Table 3) that are commonly used for describing the thin-layer drying behavior. The moisture ratio (*MR*) of the tomato slices during drying experiments was calculated by using the following Eq. (4):

$$MR = \frac{M_t - M_e}{M_0 - M_e} \tag{4}$$

where $M_t$, $M_0$ and $M_e$ are moisture content at any time, initial moisture content, equilibrium moisture content (kg water/kg dry matter), respectively, and t is drying time (min). The equilibrium moisture content ($M_e$) is relatively small compared with $M_0$, especially for infrared drying. Therefore, $M_e$ was numerically set to zero in this study. So *MR* can be simplified to [16, 17]:

$$MR = \frac{M_t}{M_0} \tag{5}$$

The drying rate (*DR*) calculated from the change in moisture content, which occurred in each consecutive time interval, were computed using Eq. (6):

$$DR = \frac{M_t - M_{t+\Delta t}}{\Delta t} \tag{6}$$

where $M_{t+\Delta t}$ is moisture content at $t + \Delta t$ (kg water/kg dry matter), and t is time (min).

#### 3.2.1 Data analysis

Data were analyzed using Statistica 8.0.550 (StatSoft Inc., Tulsa, OK, USA) software package. Non-linear least square regression analysis was used to evaluate the parameters of the selected model with the Levenberg–Marquardt algorithm. The fitting quality of the experimental data to all models was evaluated using the coefficient of determination ($R^2$), mean relative percent error (*P*), reduced Chi square ($\chi^2$), and root mean square error (*RMSE*). The $R^2$, *P*, $\chi^2$ and RMSE were calculated from following formulas:

$$R^2 = 1 - \frac{\sum \left(MR_{pre,i} - MR_{\exp,i}\right)^2}{\sum_{i=1}^{N} \left(\overline{MR}_{pre} - MR_{\exp,i}\right)^2} \tag{7}$$

$$P = \frac{100}{N} \sum_{i=1}^{N} \frac{|MR_{\exp,i} - MR_{pre,i}|}{MR_{\exp,i}} \tag{8}$$

$$\chi^2 = \frac{\sum_{i=1}^{N} \left(MR_{\exp,i} - MR_{pre,i}\right)^2}{N - z} \tag{9}$$

$$RMSE = \left[\frac{1}{N} \sum_{i=1}^{N} \left(MR_{pre,i} - MR_{\exp,i}\right)^2\right]^{1/2} \tag{10}$$

where $MR_{exp,i}$ and $MR_{pre,i}$ are experimental and predicted dimensionless moisture ratios, respectively; *N* is number of observations; *z* is number of constants. The best model was chosen based on the following four criteria: the highest value of $R^2$ and the least values of *P*, $\chi^2$ and *RMSE* [17, 19].

#### 3.2.2 Determination of effective moisture diffusivity

Fick's second law of diffusion equation was used to fit the experimental drying data for the determination of effective moisture diffusivity coefficients:

$$\frac{\partial M}{\partial t} = \nabla \left[D_{eff} (\nabla M)\right] \tag{11}$$

The solution of diffusion equation for infinite slab given by Crank [13], and supposed uniform initial moisture distribution, negligible external resistance, constant diffusivity and negligible shrinkage, is:

$$MR = \frac{8}{\pi^2} \sum_{n=0}^{\infty} \frac{1}{(2n+1)^2} \exp\left(-\frac{(2n+1)^2 \pi^2 D_{eff} t}{4L^2}\right) \tag{12}$$

where $D_{eff}$ is the effective moisture diffusivity ($m^2/s$), t is the time (s), L is the half-thickness of samples (m) and n is the summation index (ranging from 0 to infinity). For long drying periods, the above equation can be simplified to only first term of series, without much affecting the accuracy of the prediction:

$$MR = \frac{8}{\pi^2} \exp\left(-\frac{\pi^2 D_{eff} t}{4L^2}\right) \tag{13}$$

The effective moisture diffusivity ($D_{eff}$) was also calculated typically by using the slope of Eq. (13). A straight line with a slope was obtained when ln (*MR*) was plotted versus time:

$$slope = \frac{\pi^2 D_{eff}}{4L^2} \tag{14}$$

Using the slope value (Eq. 14), the effective moisture diffusivity could be determined.

#### 3.2.3 Computation of activation energy

The relationship between the effective moisture diffusivity and drying temperature was described using the Arrhenius-type equation:

$$\mathrm{D_{eff}} = \mathrm{D_0} \exp\left(-\frac{E_a}{RT}\right) \tag{15}$$

**Table 4** Calculated mean COP and SMER values at three drying air temperatures

| Drying temperature (°C) | $COP_{sys,mean}$ | SMER (kg/kWh) |
|---|---|---|
| 35 | 2.323 | 0.214 |
| 40 | 2.682 | 0.242 |
| 45 | 2.706 | 0.324 |

Here $D_0$ is the pre-exponential factor ($m^2/s$), $E_a$ is the activation energy (kJ/mol), $R$ is the universal gas constant (kJ/mol K), and $T$ is drying air temperature (K).

### 3.3 Uncertainty analysis

Uncertainty analysis is needed to validate the accuracy of the experiments. The uncertainty analysis for this study was performed using the method described by Holman [23] to define the accuracy of measured and calculated values.

$$U_F = \left[\left(\frac{\partial F}{\partial z_1}u_1\right)^2 + \left(\frac{\partial F}{\partial z_2}u_2\right)^2 + \cdots + \left(\frac{\partial F}{\partial z_n}u_n\right)^2\right]^{1/2} \quad (16)$$

In this study, the pressures, temperatures, humidifies, velocities and mass were measured with appropriate instruments.

## 4 Results and discussion

### 4.1 System performance

Experiments were carried out at 24.5 °C outdoor temperature and 53% relative humidity conditions. During the experiments, the higher SMER values were obtained for 2 h, then they decreased depend on drying rate. The highest SMER value was obtained as 0.324 kg/kWh at 45 °C drying air temperature, while the lowest value was obtained as 0.214 kg/kWh at 35 °C drying air temperature. Mean SMER and COP values were calculated as seen from Table 4.

### 4.2 Drying curves

The effect of air temperature on drying curves of the tomato slices during drying is shown in Fig. 2. The drying curves are typical to ones for similar vegetables and fruits. The moisture content decreased exponentially with elapsed duration of drying and decreased faster at higher air temperatures in all cases, as expected. The results showed that drying time decreased greatly when the temperature increased. The drying time required reaching the final moisture content of the samples were 720, 600 and 420 min

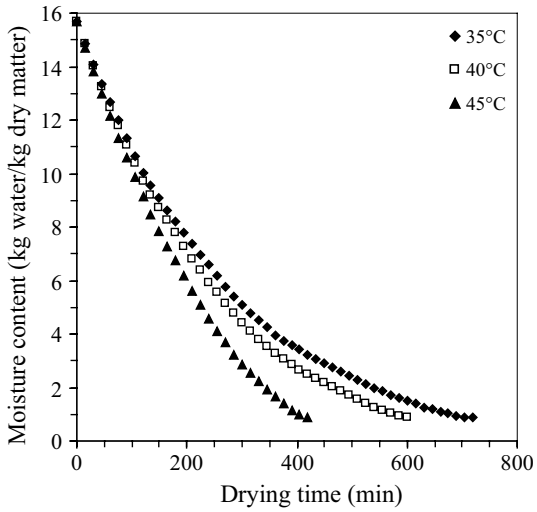


**Fig. 2** Drying curves of tomato slices at different air temperatures

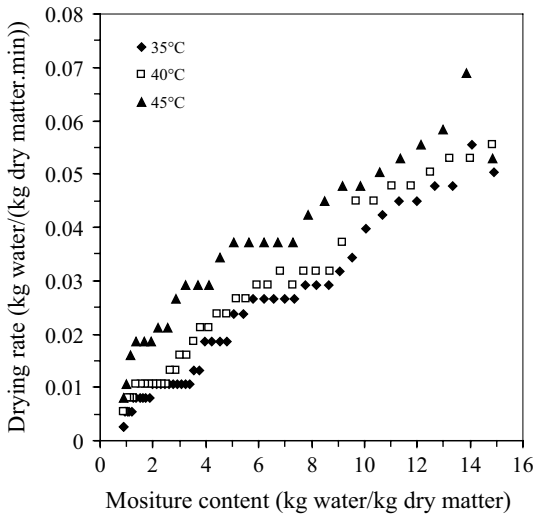


**Fig. 3** Variation of drying rate as a function of moisture content at different drying temperatures

at the temperatures of 35, 40 and 45 °C, respectively. The average drying rate samples increased 1.71 times, respectively, as air temperature increased from 35 to 45 °C. As expected, at higher air temperature, the higher heat absorption resulted in higher product temperature, higher mass transfer driving force, faster drying rate and consequently lesser drying time [30].

The drying rate curves of tomato slices are shown in Fig. 3. It is clear that the drying rate decreases continuously with moisture content. The drying rates were higher in the beginning of the process, and then decreased with a decrease in moisture content of the samples. Tomato slices did not exhibit a constant drying rate period and all the drying operations are seen to occur in the falling drying rate

**Table 5** Statistical results obtained from the selected models

| Temperature (°C) | Model name | $R^2$ | P | $\chi^2$ | RMSE |
|---|---|---|---|---|---|
| 35 | Lewis | 0.9989 | 5.1990 | 0.000078 | 0.050892 |
| | Henderson and Pabis | 0.9991 | 4.4295 | 0.000060 | 0.042585 |
| | Logarithmic | 0.9997 | 1.4592 | 0.000016 | 0.022165 |
| | Verma et al. | 0.9997 | 1.5146 | 0.000016 | 0.022739 |
| | Page | 0.9996 | 2.9082 | 0.000028 | 0.031825 |
| | Midilli et al. | 0.9998 | 1.4539 | 0.000016 | 0.021839 |
| | Parabolic | 0.9955 | 8.8204 | 0.000339 | 0.108688 |
| | Wang and Singh | 0.9920 | 12.2023 | 0.000595 | 0.144534 |
| | Weibull | 0.9996 | 2.9082 | 0.000028 | 0.031825 |
| | Aghbashlo et al. | 0.9997 | 1.9589 | 0.000017 | 0.024354 |
| 40 | Lewis | 0.9959 | 9.9940 | 0.000311 | 0.102334 |
| | Henderson and Pabis | 0.9972 | 7.9241 | 0.000216 | 0.080386 |
| | Logarithmic | 0.9997 | 1.9313 | 0.000025 | 0.025330 |
| | Verma et al. | 0.9996 | 2.4792 | 0.000028 | 0.027304 |
| | Page | 0.9993 | 3.1207 | 0.000048 | 0.036372 |
| | Midilli et al. | 0.9997 | 1.2465 | 0.000017 | 0.020406 |
| | Parabolic | 0.9982 | 5.6432 | 0.000145 | 0.060568 |
| | Wang and Singh | 0.9970 | 7.4780 | 0.000233 | 0.078413 |
| | Weibull | 0.9993 | 3.1207 | 0.000048 | 0.036372 |
| | Aghbashlo et al. | 0.9998 | 1.2302 | 0.000012 | 0.018330 |
| 45 | Lewis | 0.9818 | 21.6041 | 0.001542 | 0.185309 |
| | Henderson and Pabis | 0.9866 | 18.1459 | 0.001174 | 0.156845 |
| | Logarithmic | 0.9955 | 3.0998 | 0.000040 | 0.026512 |
| | Verma et al. | 0.9972 | 8.1577 | 0.000250 | 0.069794 |
| | Page | 0.9969 | 7.8392 | 0.000269 | 0.073984 |
| | Midilli et al. | 0.9997 | 2.3144 | 0.000028 | 0.021956 |
| | Parabolic | 0.9999 | 0.8175 | 0.000007 | 0.011539 |
| | Wang and Singh | 0.9998 | 0.9328 | 0.000011 | 0.014475 |
| | Weibull | 0.9969 | 7.8393 | 0.000269 | 0.073984 |
| | Aghbashlo et al. | 0.9998 | 1.2249 | 0.000014 | 0.016659 |

period. These results are in good agreement with those in earlier studies of tomatoes [14, 26, 30, 32].

### 4.3 Evaluation of the models

The experimental drying kinetics data at each temperature was fitted to the ten different models summarized in Table 3. The best model selected based on the highest $R^2$ and the lowest $P$, $\chi^2$ and $RMSE$ values. Results of the statistical computing are shown in Table 5. The $R^2$ values for all models were above 0.9800, while these values for Lewis model were the lowest ones. The statistical parameter estimations showed that $R^2$, $P$, $\chi^2$ and $RMSE$ values were ranged from 0.9800 to 0.9999, 0.8175 to 21.6041, 0.000007 to 0.001542, and 0.0111539 to 0.185309, respectively. Among ten models, the Midilli et al. [27], Aghbashlo et al. and Parabolic models were the best in describing the drying process of tomato slices, with the highest $R^2$ and lowest $P$, $\chi^2$ and $RMSE$ for 35, 40 and 50 °C, respectively.

To validate the selected models, plots of experimental $MR$ and predicted $MR$ by the selected models are shown in Fig. 4. Obviously, a good agreement was observed between experimental and predicted $MR$ values. That is, the data points are

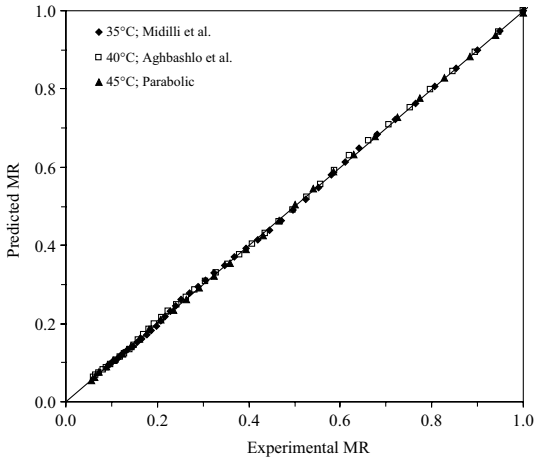


**Fig. 4** Experimental and predicted moisture ratio values at different air temperature for the proposed models

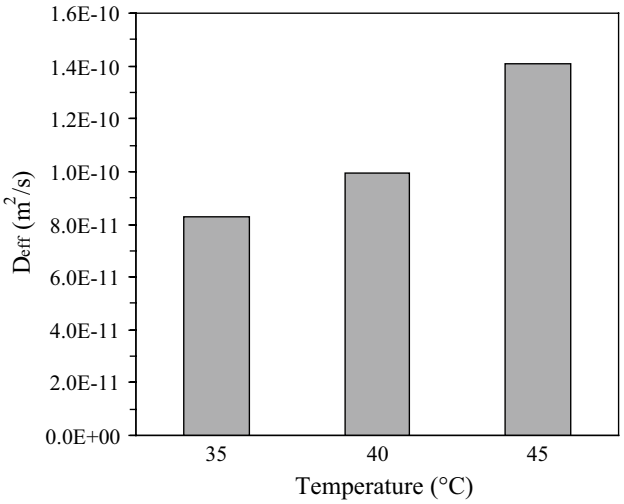


**Fig. 5** Effective moisture diffusivity versus air temperature

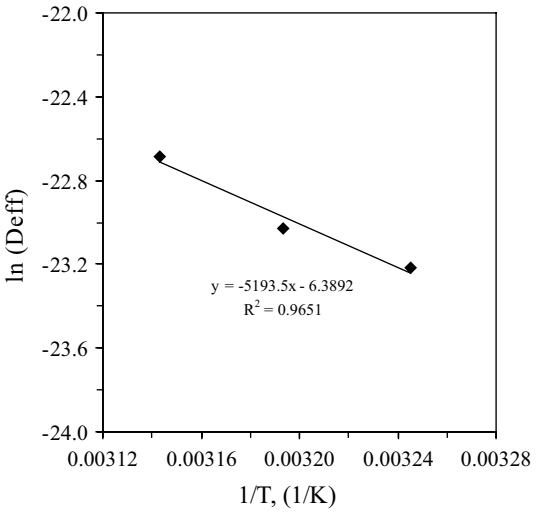


**Fig. 6** Arrhenius-type relationship between effective moisture diffusivity and air temperature

generally banded around a 45° straight line on the plots. This trend provides extra evidence for the suitability of the model to forecast the drying characteristics of tomato slices.

#### *4.3.1 Effective moisture diffusivity*

The determined values of the effective moisture diffusivity are shown in Fig. 5 and were in range between $8.28 \times 10^{-11}$ and $1.41 \times 10^{-10}$ $m^2/s$. As expected that the effective moisture diffusivity increased greatly with increasing drying temperature. The values of $D_{eff}$ obtained from this study are within the general range from $10^{-12}$ to $10^{-8}$ $m^2/s$ for biological materials [41]. The calculated values of $D_{eff}$ were consistent with the values given in literature such as Abano et al. [1] and found between $7.22 \times 10^{-9}$ and $25.19 \times 10^{-9}$ $m^2/s$ for tomato slices by using combined microwave-vacuum drying, Bagheri et al. [8] found between $3.42 \times 10^{-9}$ and $8.69 \times 10^{-9}$ $m^2/s$ for tomato slices by using open sun drying and Bennamoun et al. [9] found between $3 \times 10^{-10}$ and $5 \times 10^{-10}$ $m^2/s$ for cherry tomato by using convective drying. The differences between the results can be explained by effect of type, slice thickness, composition, and tissue characteristics of the tomatoes and the proposed model used for calculation.

#### *4.3.2 Activation energy*

The activation energy was calculated by plotting *ln* ($D_{eff}$) versus the reciprocal of the temperature (1/T), and presented in Fig. 6. Equation (17) shows the effect of temperature on $D_{eff}$ of the samples with following coefficients:

$$D_{eff} = 1.6796 \times 10^{-3} \exp\left(-\frac{5193.5}{T}\right) \quad \left(R^2 : 0.9651\right) \tag{17}$$

Using Eq. (17), the value of activation energy was found to be 43.12 kJ/mol. The values obtained in this study are in the range of 12.7–110 kJ/mol for various foods reported by Zogzas et al. [41].

## 5 Conclusions

The drying characteristics of tomato slices were investigated in a closed loop HPD system at three different drying air temperatures. The drying rate was significantly influenced by drying temperature. The drying time decreased with the increase in drying temperature. The drying of tomato slices at each temperature occurred in falling-rate period; no constant-rate period of drying was observed. To explain the drying kinetics of tomato slices, ten thin-layer drying models were applied. Statistical analysis showed that the models by Midilli et al. [27], Aghbashlo et al., and Parabolic have the best-fit quality. The effective moisture diffusivity was computed from Fick's second law, the values of which varied between $8.28 \times 10^{-11}$ and $1.41 \times 10^{-10}$ $m^2/s$, over the temperature range. With the increase of drying temperature, the effective moisture diffusivity increased. Activation energy was estimated by an Arrhenius type equation and found to be 43.12 kJ/mol. During the drying process, mean SMER as 0.324 kg/kWh and COP as 2.71 were obtained at the highest drying air temperature (45 °C).

**Acknowledgements** The authors wish to extend their thanks to the Yalova University Scientific Research Projects Coordination Unit for their support of Project No. 2013/BAP/082 entitled "Investigation Regarding the Quality and Energy Efficiency of the Use of the Heat Pump in The Drying of Agricultural Products" and to the Laboratory of the Atatürk Horticultural Research Institute which was opened for their use.

## References

1. Abano EE, Ma H, Qu W (2012) Influence of combined microwave-vacuum drying on drying kinetics and quality of dried tomato slices. J Food Qual 35:159–168
2. Abuşka M, Doğan H (2010) Endüstriyel tip ısı pompalı kurutucuda çekirdeksiz üzümün kurutulması. Politeknik Dergisi 13(4):271–279
3. Achariyaviriya S, Sopanronnarit S, Terdyothin A (2000) Mathematical model development and simulation of heat pump fruit dryer. Dry Technol 18(1–2):479–591
4. Aghbashlo M, Kianmehr MH, Khani S, Ghasemi M (2009) Mathematical modeling of carrot thin-layer drying using new model. Int Agrophys 23:313–317

5. Aktas M, Sevik S, Doğan H, Ozturk M (2012) Fotovoltaik ve termal günes enerjili sürekli bir kurutucuda domates kurutulması. J Agric Sci 18:287–298
6. Aktas M, Kara MÇ (2013) Güneş Enerjisi ve Isı Pompalı Kurutucuda Dilimlenmiş Kivi Kurutulması. J Fac Eng Archit Gazi Univ 28(4):733–741
7. Aktas M, Ceylan I, Yılmaz S (2009) Determination of drying characteristics of apples in a heat pump and solar dryer. Desalination 239:266–275
8. Bagheri H, Arabhosseini A, Kianmehr MH, Chegini GR (2013) Mathematical modeling of thin layer solar drying of tomato slices. Agric Eng Int CIGR J 15:146–153
9. Bennamoun L, Khama R, Léonard A (2015) Convective drying of a single cherry tomato: modeling and experimental study. Food Bioprod Process 94:114–123
10. Ceylan I (2009) Energy analysis of PID controlled heat pump dryer. Engineering 1:188–195
11. Chua K, Mujumdar A, Hawlader M, Chou S, Ho J (2001) Batch drying of banana pieces-effect of stepwise change in drying air temperature on drying kinetics and product colour. Food Res Int 34(8):721–731
12. Colak N, Hepbaslı A (2009) A review of heat pump drying part 1-systems models and stuides. Energy Convers Manag 50:2180–2186
13. Crank J (1975) The mathematics of diffusion. Oxford University Press, London
14. Doymaz I (2007) Air drying characteristics of tomatoes. J Food Eng 78(4):1291–1297
15. El-Sebaii AA, Aboul-Enein S, Ramadan MRI, El-Gohary HG (2002) Empirical correlations for drying kinetics of some fruits and vegetables. Energy 27(9):845–859
16. Faal S, Tavakoli T, Ghobadian B (2015) Mathematical modelling of thin layer hot air drying of apricot with combined heat and power dryer. J Food Sci Technol 52:2950–2957
17. Fahloul D, Lahbari M, Benmoussa H, Mezdour S (2009) Effect of osmotic dehydration on the freeze drying kinetics of apricots. J Food Agric Environ 7:117–121
18. FAO (2014) http://faostat3.fao.org/compare/E
19. Falade KO, Ogunwolu OS (2014) Modeling of drying patterns of fresh and osmotically pretreated cooking banana and plantain slices. J Food Process Preserv 38:373–388
20. Filho OA, Strommen I (1996) The application of heat pump in drying of biomaterials. Dry Technol 14(9):2061–2090
21. Hasturk Sahin F, Aktas T, Orak H, Ulger P (2011) Influence of pretreatments and different drying methods on color parameters and lycopene content of dried tomato. Bulg J Agric Sci 17:867–881
22. Hawlader MNA, Perera CO, Tian M (2006) Properties of modified atmosphere heat pump dried foods. J Food Eng 74:392–401
23. Holman JP (1994) Experimental methods for engineers, 6th edn, McGraw-Hill, Singapore City
24. Jia X, Jolly P, Clements S (1990) Heat pump assisted continuous drying part 2: simulation results. Int J Energy Res 14:771–782
25. Juan W, Chong Z, Zhentao Z, Luwei Y (2013) Performance analysis of heat pump dryer to dry mushroom. Adv J Food Sci Technol 5(2):164–168
26. Kingsly ARP, Singh R, Goyal RK, Singh DB (2007) Thin-layer drying behavior of organically produced tomato. Am J Food Technol 2:71–78
27. Midilli A, Kucuk H, Yapar Z (2002) A new model for single layer drying. Dry Technol 20:1503–1513
28. Pal US, Khan MK, Mohanty SN (2008) Heat pump drying of green sweet pepper. Dry Technol 26:1584–1590
29. Phani KA, Greg JS (2005) Re-circulating heat pump assisted continuous bed drying and energy analysis. Int J Energy Res 29:961–972
30. Ponkham K, Meeso N, Soponronnarit S, Siriamornpun S (2012) Modeling of combined far-infrared radiation and air drying of a ring shaped-pineapple with/without shrinkage. Food Bioprod Proces 90:155–164
31. Prasertsan S, Saen-Saby P (1998) Heat pump drying of agricultural material. Dry Technol 16(1–2):235–250
32. Purkayastha MD, Nath A, Deka BC, Mahanta CL (2013) Thin layer drying of tomato slices. J Food Sci Technol 50(4):642–653
33. Queiroz R, Gabas AL, Telis VRN (2004) Drying kinetics of tomato by using electric resistance and heat pump dryers. Dry Technol 22(7):1603–1620
34. Sacilik K, Keskin R, Elicin AK (2006) Mathematical modeling of solar tunnel drying of thin layer organic tomato. J Food Eng 73:231–238
35. Soponronnarit S, Nathakaranakule A, Wetchacama S, Swasdisevi T, Rukprang P (1998) Fruit drying using heat pump. RERIC Int Energy J 20:38–53
36. Strommen I, Kramer K (1994) New applications of heat pumps in drying processes. Dry Technol 12(4):889–901
37. Teeboonma U, Tiansuwan J, Soponronnarit S (2003) Optimization of heat pump fruit dryers. J Food Eng 59:369–377
38. Tosun S (2009) Bazı Tarımsal Ürünler İçin Isı Pompalı Bir Kurutucunun Geliştirilmesi ve Termodinamik Analizi. Doktora Tezi Ege Üniversitesi Fen Bilimleri Enstitüsü
39. Yun-Hong L, Shuai M, Jian-Ye W, Jian-Xue L (2014) Drying and quality characteristics of flos lonicerae in modified atmosphere with heat pump system. J Food Process Eng 37:37–45
40. Zanoni B, Peri C, Nani R, Lavell V (1998) Oxidative heat damage of tomato halves as affected by drying. Food Res Int 31(5):395–401
41. Zogzas NP, Maroulis ZB, Marinos-Kouris D (1996) Moisture diffusivity data compilation in foodstuffs. Dry Technol 14:2225–2253